Supporting Information for

"Broadband Cross Polarization for Ultra-Wideline Magic-Angle Spinning NMR"

James J. Kimball[1,2], Sophia Keil[3], Max Bußkamp[3], Adam R. Altenhof[1,2], Michael Ryan Hansen[3,4]*, and Robert W. Schurko[1,2,*]

1. Department of Chemistry & Biochemistry, Florida State University, Tallahassee, FL 32306
2. National High Magnetic Field Laboratory, Tallahassee, FL 32310
3. Institute for Physical Chemistry, University of Münster, DE-48149 Münster, Germany
4. Center for Multiscale Theory and Computation (CMTC), University of Münster, DE-48149 Münster, Germany

*Authors to whom correspondence should be addressed.
Phone: +1 850 645 8614, E-mail: rschurko@fsu.edu
Phone: +49 251 83 29161, E-mail: mhansen@uni-muenster.de

Supporting Information Provided:

Supplement S1: Synthesis of [Sn(HPDABA)]Cl_2

The novel [Sn(HPDABA)]Cl_2 (HPDABA = 2-hydroxy-4-(propan-2-ylideneamino)benzoic acid) cocrystal was prepared mechanochemically via ball milling of the dried reagents in the appropriate molar ratios: (1:1) tin (II) chloride (Sigma Aldrich) and 4-aminosalicylic acid (Sigma Aldrich) along with 30 μL of acetone. This synthesis used a MM400 Milling Media mixer mill, 10 mL stainless steel milling jars, and two 7 mm stainless steel ball bearings.

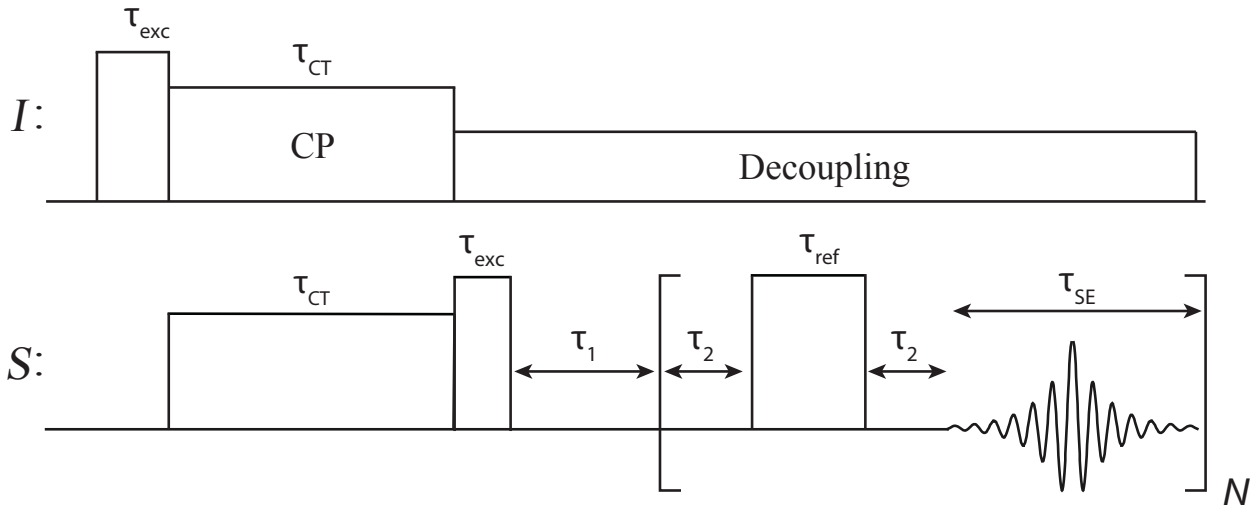

Scheme S1. Schematic representation of the CP/CPMG pulse sequence used for power calibrations. Values of τ_{cal} resulting in null signal are interpreted as those resulting in a 90° flip angle.

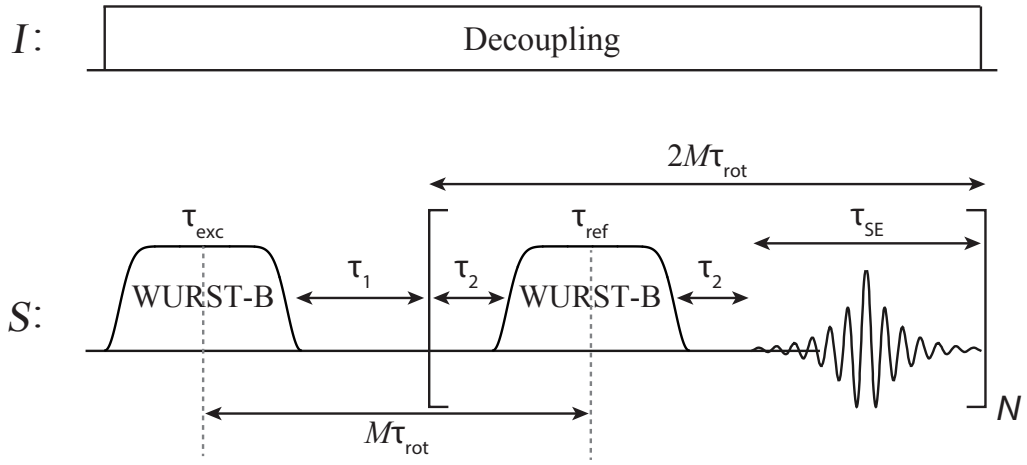

Scheme S2. Schematic representation of the WCPMG-MAS pulse sequence.

Table S1. Experimental Parameters for BRAIN-CP/WCPMG-MAS Spectra

Figure Number	1	7	8	9
Compound	[Sn(HPDABA)]Cl_2	DBTO	Cisplatin	$Rh_2Cl_2(COD)_2$
^{1}H Larmor frequency (MHz)	600	600	500	900
S Larmor frequency (MHz)	223.74	223.74	109.21	28.68
Spinning speed (kHz), ν_{rot}	15	12	25	14
Number of Transients	128	64	256	12288
Recycle Delay (s)	2	4	5	2
Dwell Time (μs)	1	1	0.8	1
Number of Meiboom-Gill loops, *N*	50	9	248	65
Spin Echo Length, τ_{SE} (μs)	250	300	100	180
Acquisition Time (ms)	20.3	31.2	39.92	28.2
Ring-Down Delay, τ_{dead} (μs)	41.7	41.7	10	88.5
^{1}H Excitation Pulse Length (μs)	2.63	2.63	2.08	4.62
^{1}H Excitation Pulse Amplitude (kHz)	95	95	120	54
^{1}H Spin-lock Power, $\nu_{1,I}$ (kHz)	34	17	43.5	35
Contact Pulse Length, τ_{CT} (ms)	10	10	20	20
WURST-A sweep width, $\Delta\nu_A$ (kHz)	15	12	25	14
WURST-A amplitude, $\nu_{1,A}$ (kHz)	15	12	25	14
WURST-A shape parameter, *N*	20	20	2	20
WURST-B length, τ_B (μs)	67	83	40	72
WURST-B sweep width, $\Delta\nu_B$ (kHz)	1600	1800	3500	1200
WURST-B amplitude, $\nu_{1,B}$ (kHz)	40.3	38.2	78.1	33.7
WURST-B shape parameter, *N*	20	20	2	20
WURST-C length, τ_C (μs)	67	83	50	72
WURST-C sweep width, $\Delta\nu_C$ (kHz)	1600	1800	3500	1200
WURST-C amplitude, $\nu_{1,C}$ (kHz)	40.3	38.2	5.75	33.7
WURST-C shape parameter, *N*	20	20	2	20
^{1}H TPPM Decoupling RF Power (kHz)	50	50	82.78	50
Spectral Width (kHz)	1000	1000	1250	1000

Table S2. Experimental Parameters for WCPMG-MAS Spectra

Figure Number	1	8
Compound	[Sn(HPDABA)]Cl_2	Cisplatin
^{1}H Larmor frequency (MHz)	600	500
S Larmor frequency (MHz)	223.74	109.21
Spinning speed (kHz), ν_{rot}	15	25
Number of Transients	128	256
Recycle Delay (s)	200	60
Dwell Time (μs)	1	0.8
Number of Meiboom-Gill loops, *N*	50	248
Spin Echo Length, τ_{SE} (μs)	250	100
Acquisition Time (ms)	20.3	39.92
Ring-Down Delay, τ_{dead} (μs)	41.7	10
WURST-B length, τ_B (μs)	67	40
WURST-B sweep width, $\Delta\nu_B$ (kHz)	1600	3500
WURST-B amplitude, $\nu_{1,B}$ (kHz)	40.3	78.1
WURST-B shape parameter, *N*	20	2
WURST-C length, τ_C (μs)	67	50
WURST-C sweep width, $\Delta\nu_C$ (kHz)	1600	500
WURST-C amplitude, $\nu_{1,C}$ (kHz)	40.3	5.75
WURST-C shape parameter, *N*	20	2
^{1}H TPPM Decoupling RF Power (kHz)	50	82.78
Spectral Width (kHz)	1000	1250

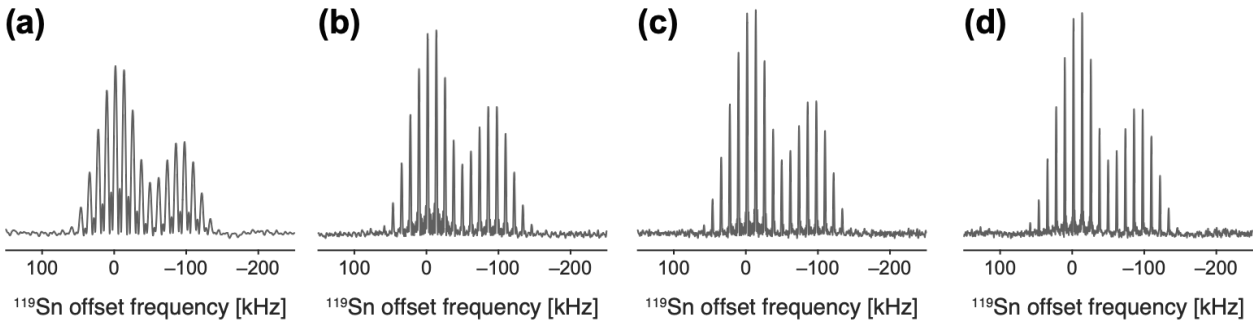

Figure S1. ^{1}H-^{119}Sn BRAIN-CP/WCPMG-MAS powder patterns of DBTO acquired at 14.1 T at ν_{rot} = 12 kHz with τ_{SE} = (a) 200 μs, (b) 600 μs, (c) 800 μs, and (d) 1000 μs. For each experiment, the total acquisition time was held constant at 30 ms by varying the number of CPMG loops.

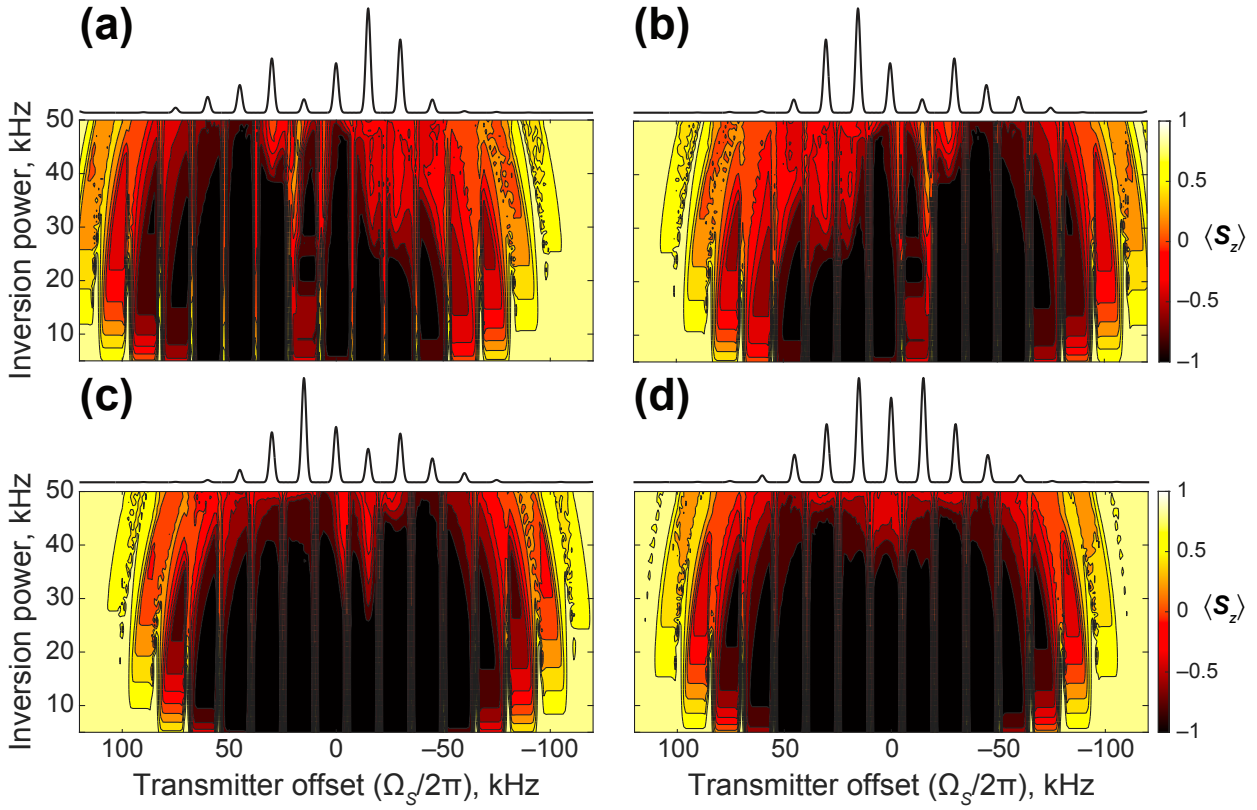

Figure S2. Contour plots showing SIMPSON simulations of $\langle \mathbf{S}_z \rangle$ as a function of $\nu_{1,S}$ and $\Omega_S/2\pi$ (both in increments of 1 kHz) at the end of a S^{3}AP inversion pulse for a one-spin system with the CSA described by δ_{iso} = 0 ppm, Ω_{CS} = 675 ppm, and (a) κ = –1, (b) κ = +1, (c) κ = 0.5, and (d) κ = 0, all using the Herzfeld-Berger convention. The starting density matrix is $\rho(0) = +\langle \mathbf{S}_z \rangle$. In all cases, $\Delta = \nu_{rot}$ = 15 kHz and the pulse length τ_{pulse} = 10 ms. Powder averaging in each simulation is accomplished using the REPULSION scheme, using 100 β and 10 γ orientations. Ideal spectra are displayed above each contour plot.

Supplement S2: Jolting frame representation of a spin-1/2 nucleus with an anisotropic CS

Following the work of Pell *et al*., we demonstrate the ability to represent an anisotropic CS interaction for a single spin isochromat under MAS as a Fourier series, which can subsequently be used to define the jolting frame transformation. We make use of the Haeberlen convention in the description of the CS tensor with the principal components defined such that $|\delta_{zz} - \delta_{iso}| \geq |\delta_{yy} - \delta_{iso}| \geq |\delta_{xx} - \delta_{iso}|$, where $\delta_{iso} = (\delta_{xx} + \delta_{yy} + \delta_{zz})/3$ is the isotropic chemical shift, $\delta = \delta_{zz} - \delta_{iso}$ is the reduced anisotropy, and $\eta = (\delta_{yy} - \delta_{xx})/\delta$ is the asymmetry parameter.

The chemical shift frequency for a single spin isochromat can be described using rank-zero and rank-two irreducible spherical tensor (IST) components, which are given by:[1]

$$A_{00} = -\frac{1}{\sqrt{3}}\delta_{iso} \qquad A_{20}^{P} = \sqrt{\frac{3}{2}}\delta \qquad A_{2\pm2}^{P} = -\frac{1}{2}\eta\delta \tag{S1}$$

where the superscript 'P' denotes the PAS. The spin components are:

$$T_{00} = -\frac{1}{\sqrt{3}}\,\mathbf{I}_z B_0 \qquad T_{20} = \frac{1}{\sqrt{6}}\mathbf{I}_z B_0 \tag{S2}$$

The isotropic and reduced anisotropy terms are represented in frequency units such that $\omega_{iso} = \omega_0\delta_{iso}$ and $\omega_{aniso} = \omega_0\delta$, where ω_0 is the Larmor frequency. The benefit of using ISTs is in the compact description of their transformations under rotation expressed in some frame 'F' as:[2]

$$A_{2m}^{F} = \sum_{p=-2}^{+2} A_{2p}^{P} D_{pm}^{2}(\alpha, \beta, \gamma) \tag{S3}$$

where D_{pm}^{2} is a second-rank Wigner rotation matrix, and α, β, and γ are the Euler angles defining active rotation from the frame 'P' to frame 'F'. Under stationary conditions, the chemical shift frequency is the sum of the isotropic and anisotropic terms, and can be written in the laboratory frame as:

$$\omega_{CS} = A_{00}T_{00} + A_{20}^{L}T_{20} \tag{S4}$$

The A_{00} term is not affected by rotations and is thus of lesser interest than the A_{20}^{P} term, which is expressed in the laboratory frame, "L", as

$$A_{20}^{\mathrm{L}} = \sum_{p=-2}^{+2} A_{2p}^{\mathrm{P}} D_{p0}^{2}(\alpha, \beta, \gamma) \tag{S5}$$

Under MAS, a transformation into the rotor frame is required before the transformation expressed in **eq. S5**. The final IST component in the laboratory frame is then written as:

$$A_{20}^{\mathrm{L}} = \sum_{p=-2}^{+2} \sum_{q=-2}^{+2} A_{2p}^{\mathrm{P}} D_{qp}^{2}(\alpha, \beta, \gamma) D_{p0}^{2}(0, \phi_{\mathrm{rot}}, -\omega_{\mathrm{rot}} t) \tag{S6}$$

where $\phi_{\mathrm{rot}} = \tan^{-1}(\sqrt{2})$ is the magic angle. **Eq. S6** can be simplified to:

$$A_{20}^{\mathrm{L}} = \sum_{p=-2}^{+2} \sum_{q=-2}^{+2} A_{2p}^{\mathrm{P}} D_{qp}^{2}(\alpha, \beta, \gamma) d_{p0}^{2}(\phi_{\mathrm{rot}}) \exp(ip\omega_{\mathrm{rot}} t) \tag{S7}$$

where $d_{p0}^{2}(\phi_{\mathrm{rot}})$ is a small-*d* Wigner matrix. **Eq. S7** is a Fourier series, which can be expressed as:[3]

$$\Omega_{\mathrm{CS}}(t, \alpha, \beta, \gamma) = \sum_{p=-2}^{+2} \omega_{p}(\alpha, \beta, \gamma) \exp(ip\omega_{\mathrm{rot}} t) \tag{S8}$$

where $\Omega_{\mathrm{CS}}(t, \alpha, \beta, \gamma) \equiv A_{20}^{\mathrm{L}}$ and $\omega_{p}(\alpha, \beta, \gamma) \equiv \sum_{q=-2}^{+2} A_{2p}^{\mathrm{P}} D_{qp}^{2}(\alpha, \beta, \gamma) d_{p0}^{2}(\phi_{\mathrm{rot}})$. The operator describing the transformation into the jolting frame is given by:

$$\mathbf{U}(t) = \exp(-i\Phi_{CS}(t, \alpha, \beta, \gamma)\mathbf{I}_{z}) \tag{S9}$$

where

$$\Phi_{\mathrm{CS}}(t, \alpha, \beta, \gamma) = \int_{0}^{\tau_{\mathrm{rot}}} \Omega_{CS}(t, \alpha, \beta, \gamma) dt \tag{S10}$$

The periodicity of the above equation allows for an expansion as a Fourier series:[4,5]

$$\exp\left(i\Phi_{\mathrm{CS}}(\beta, \gamma, t)\right) = \sum_{m=-\infty}^{+\infty} B_{m}(\beta) \exp\left(i\phi_{m}(\gamma)\right) \exp(im\omega_{\mathrm{rot}} t) \tag{S11}$$

where $\sum_{m=-\infty}^{=\infty} B_{m}(\beta) = 1$ are the Fourier coefficients and the $\exp(i\phi_{m}(\gamma))$ terms describe the phase of the *m*th SSB. The coefficients B_m are solved analytically as:

$$B_{m}(\beta) \exp\left(i\phi_{m}(\gamma)\right) = \frac{1}{\tau_{\mathrm{rot}}} \int_{0}^{\tau_{\mathrm{rot}}} \exp(i\Phi_{\mathrm{CS}}(\beta, \gamma, t)) \exp(-im\omega_{\mathrm{rot}} t)\, dt \tag{S12}$$

The Hamiltonian describing the application of a S^3AP to a single spin-1/2 nucleus with an anisotropic chemical shift under MAS in the FM frame can be represented as:[6,7]

$$\mathbf{H}_S^{\mathrm{FM}}(\beta,\gamma,t) = \left[\Omega_S - \omega_{\mathrm{p}}(t) + \Omega_{\mathrm{CS}}(\beta,\gamma,t)\right]\mathbf{S}_z + \omega_{1,S}A(t)\mathbf{S}_x \tag{S13}$$

where $\Omega_{CS}(\beta,\gamma,t)$ is the orientation-dependent chemical shift given by **eq. S8**, $\omega_p(t) = d\varphi(t)/dt$ is the instantaneous (*i.e.*, time-dependent) transmitter frequency arising from the phase modulation, $\varphi(t) = \pm 2\pi\{(\Delta/2)t - (\Delta/2\tau_{CT})t^2\}$, and $A(t) = 1 - |\cos(\pi t/\tau_{CT})|^N$ is the amplitude modulation (here N is an integer, commonly set to 2, 20, or 80; herein, values of 2 or 20 are used), and τ_{CT} is the contact pulse length.

Transformation from the FM frame into the J-frame is accomplished by the operator $\mathbf{R}_z^{\mathrm{J}} = \exp(i\Phi_{\mathrm{CS}}(\beta,\gamma,t)\mathbf{S}_z)$ and the new Hamiltonian is written as

$$\mathbf{H}_S^{\mathrm{J}}(t,\beta,\gamma) = \sum_{m=-\infty}^{+\infty}\left(\Omega_S - \omega_{\mathrm{p}}(t)\right)\mathbf{S}_z \tag{S14}$$

$$+\omega_{1,S}A(t)\exp(i\Phi_{\mathrm{CS}}(\beta,\gamma,t)\mathbf{S}_z)\mathbf{S}_x\exp(-i\Phi_{\mathrm{CS}}(\beta,\gamma,t)\mathbf{S}_z)$$

A final transformation into a frame rotating synchronously with the MAS rotation is accomplished using the operator $\mathbf{R}_z^{\mathrm{rot}} = \exp(im\omega_{\mathrm{rot}}t\mathbf{S}_z)$ and the resulting Hamiltonian is given by

$$\mathbf{H}_S^{\mathrm{J,rot}}(t,\beta,\gamma) = \sum_{m=-\infty}^{+\infty}\left(\Omega_S - m\omega_{\mathrm{rot}} - \omega_{\mathrm{p}}(t)\right)\mathbf{S}_z \tag{S15}$$

$$+\omega_{1,S}A(t)\,B_m(\beta)\exp(i\phi_m(\gamma)\mathbf{S}_z)\mathbf{S}_x\exp(-i\phi_m(\gamma)\mathbf{S}_z)$$

Such an expression allows for an interpretation of the effective frequency as

$$\omega_{\mathrm{e},S}^{\mathrm{J,rot}}(\beta,t,m) = \sum_{m=-\infty}^{+\infty}\left[\left(\Omega_S - m\omega_{\mathrm{rot}} - \omega_{\mathrm{p}}(t)\right)^2 + \left(\omega_{1,S}A(t)B_m(\beta)\right)^2\right]^{1/2}, \tag{S16}$$

which is **eq. 1** of the main text.

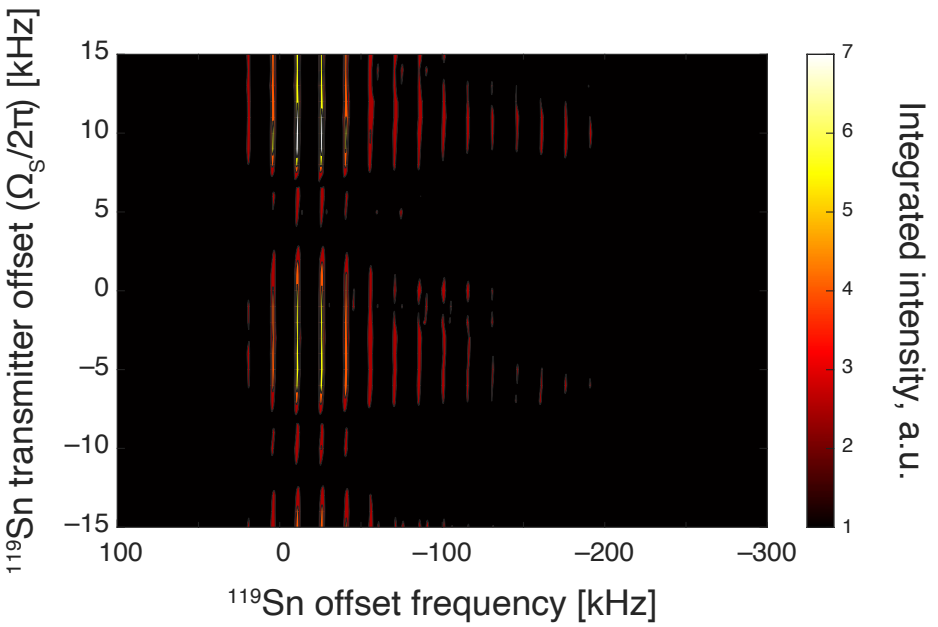

Figure S3. Contour plot showing ^{1}H-^{119}Sn BRAIN-CP/WCPMG-MAS powder patterns of [Sn(HPDABA)]Cl_2 acquired at 14.1 T as a function of $\Omega_S/2\pi$. The condition $\nu_{1,S} = \nu_{rot} = \Delta = 15$ kHz is fulfilled. In all cases, $\nu_{1,I} = 34$ kHz and $\tau_{CT} = 10$ ms.

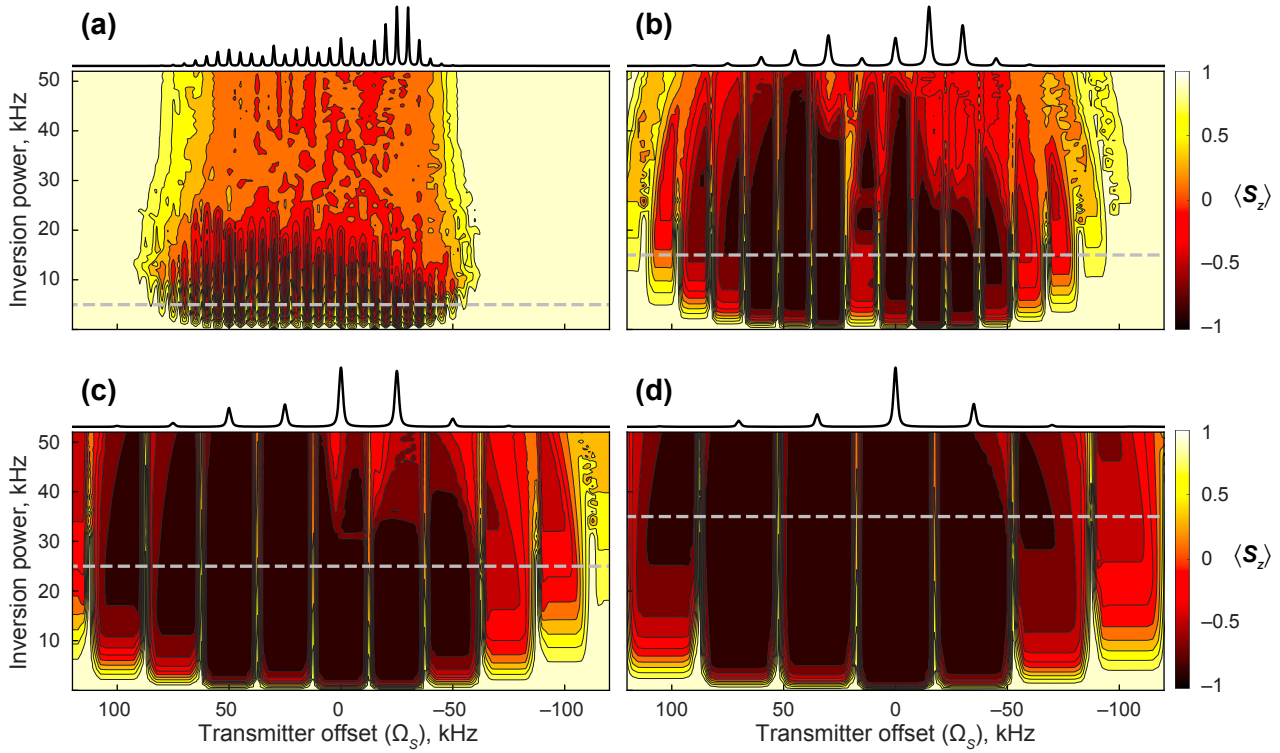

Figure S4. Contour plots showing SIMPSON simulations of $\langle \mathbf{S}_z \rangle$ as a function of $\nu_{1,S}$ and $\Omega_S/2\pi$ (both in increments of 1 kHz) at the end of a S^3AP inversion pulse for a one-spin system under MAS conditions of ν_{rot} = (a) 5 kHz, (b) 15 kHz, (c) 25 kHz, and (d) 35 kHz. The CSA is described by δ_{iso} = 0 ppm, Ω_{CS} = 675 ppm, and κ = –1 using the Herzfeld-Berger convention. The starting density matrix is $\rho(0) = +\langle \mathbf{S}_z \rangle$. In all cases, $\Delta = \nu_{1,S} = \nu_{rot}$ and the pulse length τ_{pulse} = 10 ms. Dashed lines indicate the condition where $\nu_{1,S} = \nu_{rot}$ is fulfilled. Powder averaging in each simulation is accomplished using the REPULSION scheme, using 100 β and 10 γ orientations. Ideal spectra are displayed above each contour plot.

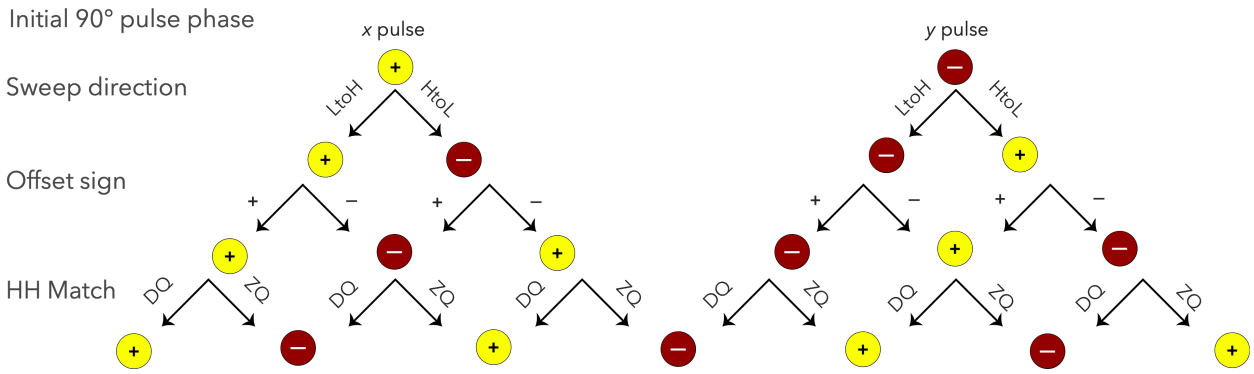

Scheme S3. Schematic representation of effects of different parameters on the sign of $\langle \mathbf{S}_z \rangle$ produced by BRAIN-CP/MAS. Colored circles represent the sign of $\langle \mathbf{S}_z \rangle$ (yellow = positive, red = negative) and arrows represent the following operations: the initial phase of the 90° pulse applied to the ^{1}H channel, the direction of the frequency sweep, the sign of the effective frequency at the time in which the match is fulfilled, and the nature of the matching condition (*i.e.*, either ZQ or DQ).

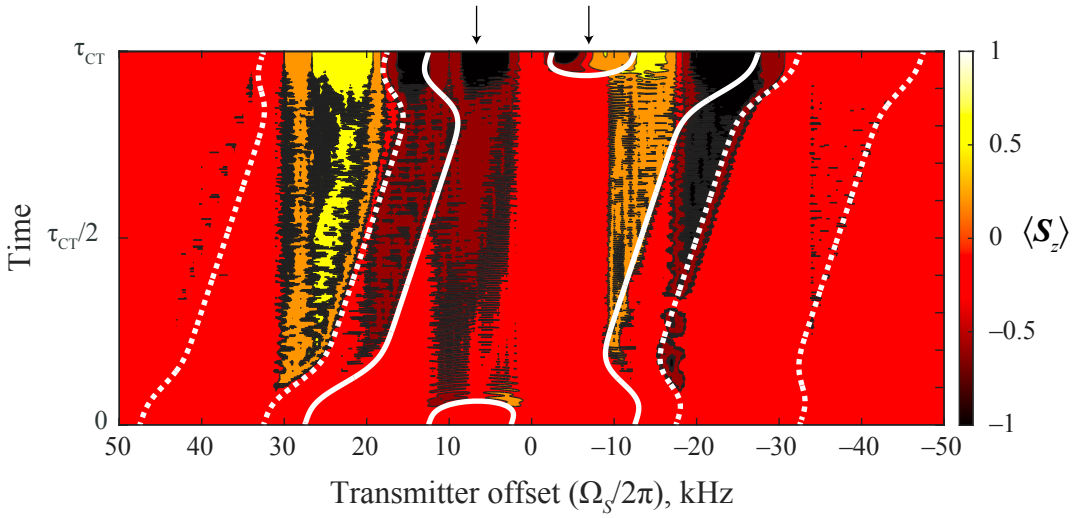

Figure S5: Numerical simulations of BRAIN-CP/MAS $I \rightarrow S$ polarization transfer for a two-spin system ($I = {}^1$H, $S = {}^{13}$C) under MAS conditions of $\nu_{rot} = 15$ kHz. The ^{13}C chemical shift tensor parameters are: $\delta_{iso} = 0$ ppm, $\Omega_{CS} = 1350$ ppm, and $\kappa = -1$. The $\beta = 0°$ isochromat is used, where β is the angle between σ_{zz} and the rotor axis. The expectation value $\langle \mathbf{S}_z \rangle$ is plotted as a function of τ_{CT} and $\Omega_S/2\pi$ for simulations wherein $\Delta = \nu_{1,S} = \nu_{rot} = 15$ kHz and $\nu_{1,I} = 10$ kHz. The heteronuclear dipolar coupling is given by $b_D^{IS}/2\pi = 4$ kHz with the dipolar vector oriented at $\theta = 45°$ relative to the rotor. Solid and dashed white lines correspond to ZQ and DQ matching conditions, respectively, as given by **eq. 5** of the main text. The region between $\pm\Delta/2$ is indicated by arrows above the contour plot.

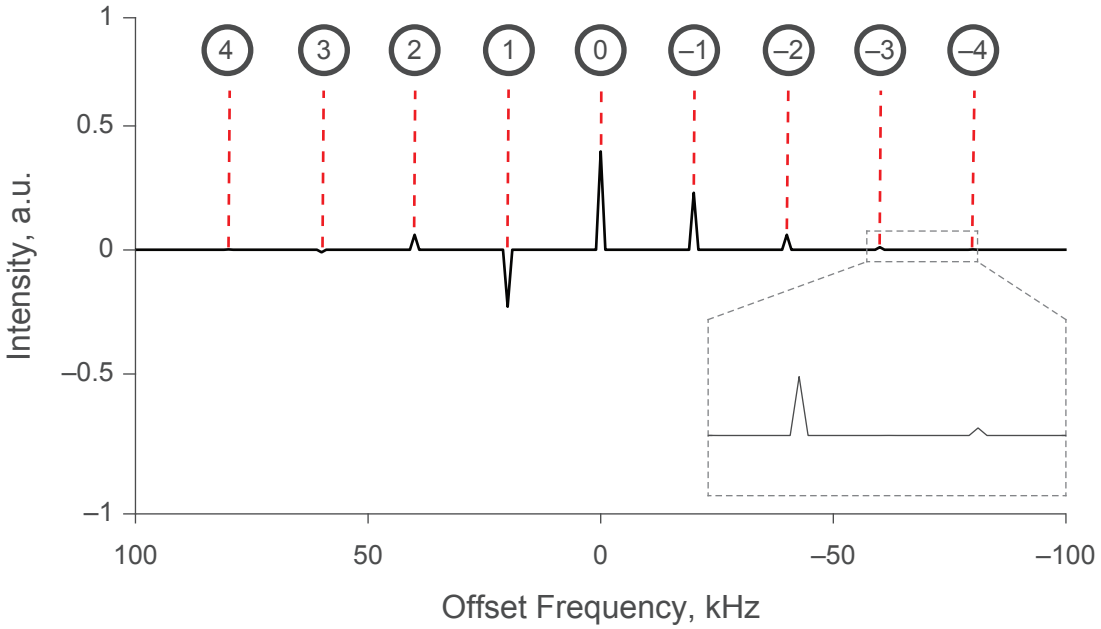

Figure S6. Ideal single-crystal MAS NMR spectrum for the β = 90° isochromat of a one–spin system with a CSA described by δ_{iso} = 0 ppm, Ω = 675 ppm, and κ = –1 using the Herzfeld-Berger convention at ν_{rot} = 10 kHz. Each of the nine SSBs with non–zero intensities are identified by the circled numbers and the corresponding intensities and offsets relative to the isotropic shift (0 kHz) for each one is displayed below in **Table S3**. The inset shows the small but non–negligible intensities of the SSBs at –60 and –80 kHz.

Sideband number	Amplitude scaling factor (B_m)	Effective transmitter offset (Ω_m, kHz)
4	1.32×10^{-3}	80
3	-1.03×10^{-2}	60
2	6.03×10^{-2}	40
1	-2.30×10^{-1}	20
0	3.96×10^{-1}	0
–1	2.30×10^{-1}	–20
–2	6.03×10^{-2}	–40
–3	1.03×10^{-2}	–60
–4	1.32×10^{-3}	–80

Table S3. Amplitude scaling factors (B_m) and transmitter offsets (Ω_m) for each component of the J-frame representation of the effective frequency, $\omega_{e,S}^{J,rot}(\beta, t, m)$, according to **eq. 6** of the main text, shown for the β = 90° isochromat in **Fig. S5**.

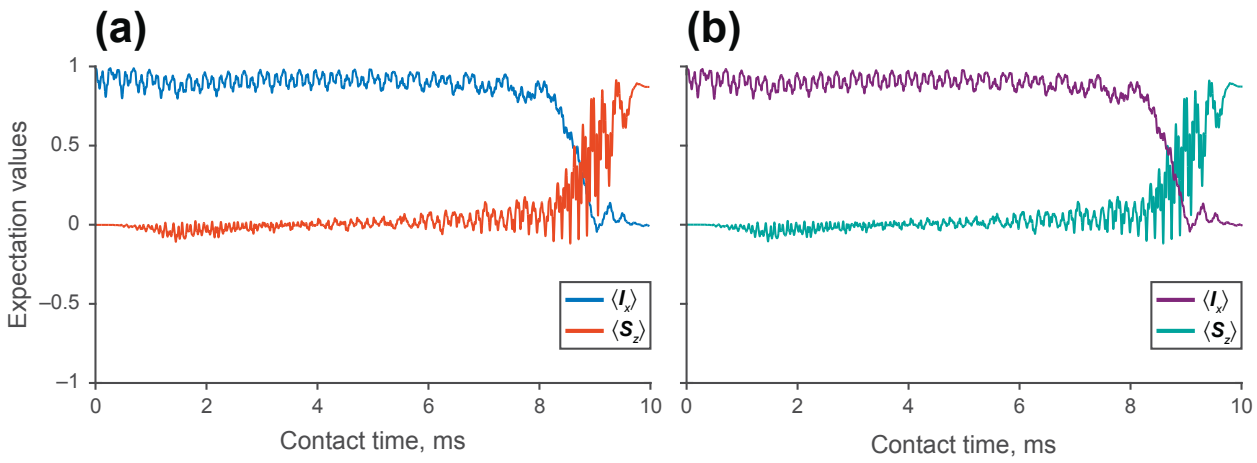

Figure S7. Numerical simulations of $I \rightarrow S$ BRAIN-CP/MAS transfer during τ_{CT} for a two-spin system using the $\beta = 90°$ isochromat whose ideal single crystal pattern is shown in **Fig. S6**. Simulations are conducted using the (a) FM frame and (b) jolting frame Hamiltonians (**eq. S13** and **eq. S15**, respectively). The terms B_m and Ω_m are given in **Table S3**. In both cases, $\nu_{rot} = \nu_{1,S} = \Delta = 10$ kHz, $\nu_{1,I} = 17$ kHz, and $b_D^{IS}/2\pi = 3.2$ kHz with the dipolar vector oriented at $\theta = 45°$ relative to the rotor.

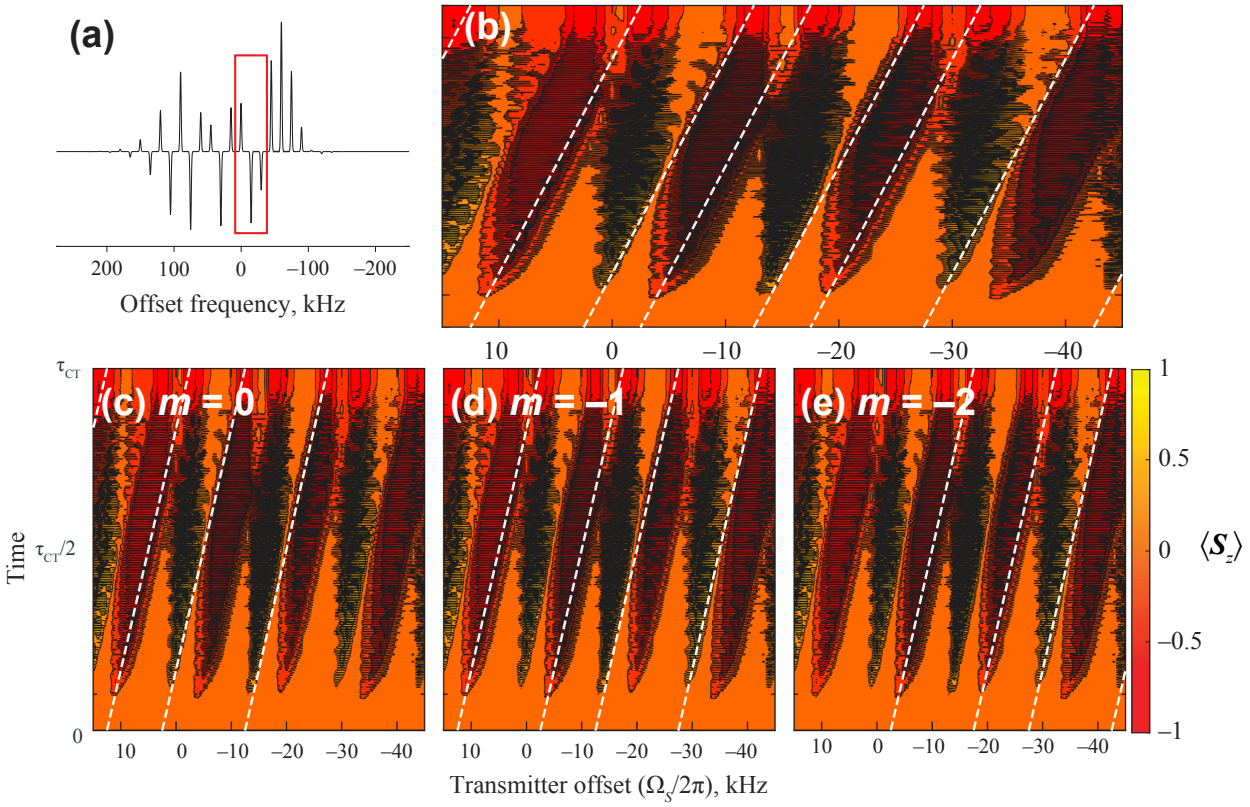

Figure S8: (a) Ideal single crystal MAS spectrum for the β = 35° isochromat, where β is the angle between σ_{zz} and the rotor axis, with a chemical shift tensor described by δ_{iso} = 0 ppm, Ω_{CS} = 1350 ppm, and κ = –1. The red box is used to highlight the m = 0, –1, and –2 SSBs. (b-e) Numerical simulations of BRAIN-CP/MAS $I \rightarrow S$ polarization transfer for a two-spin system (I = ^{1}H, S = ^{13}C) with ν_{rot} = 15 kHz. The CSA of the ^{13}C spin is that described in (a). The expectation value $\langle \mathbf{S}_z \rangle$ is plotted as a function of τ_{CT} and $\Omega_S/2\pi$ for simulations wherein $\Delta = \nu_{1,S} = \nu_{rot}$ = 15 kHz and $\nu_{1,I}$ = 10 kHz. The heteronuclear dipolar coupling is given by $b_D^{IS}/2\pi$ = 4 kHz with the dipolar vector oriented at θ = 45° relative to the rotor. Dashed white lines represent analytical solutions to **eq. 7** of the main text for (b) the m = 0, –1, and –2 SSBs, (c) the m = 0 SSB, (d) the m = –1 SSB, and (e) the m = –2 SSB.

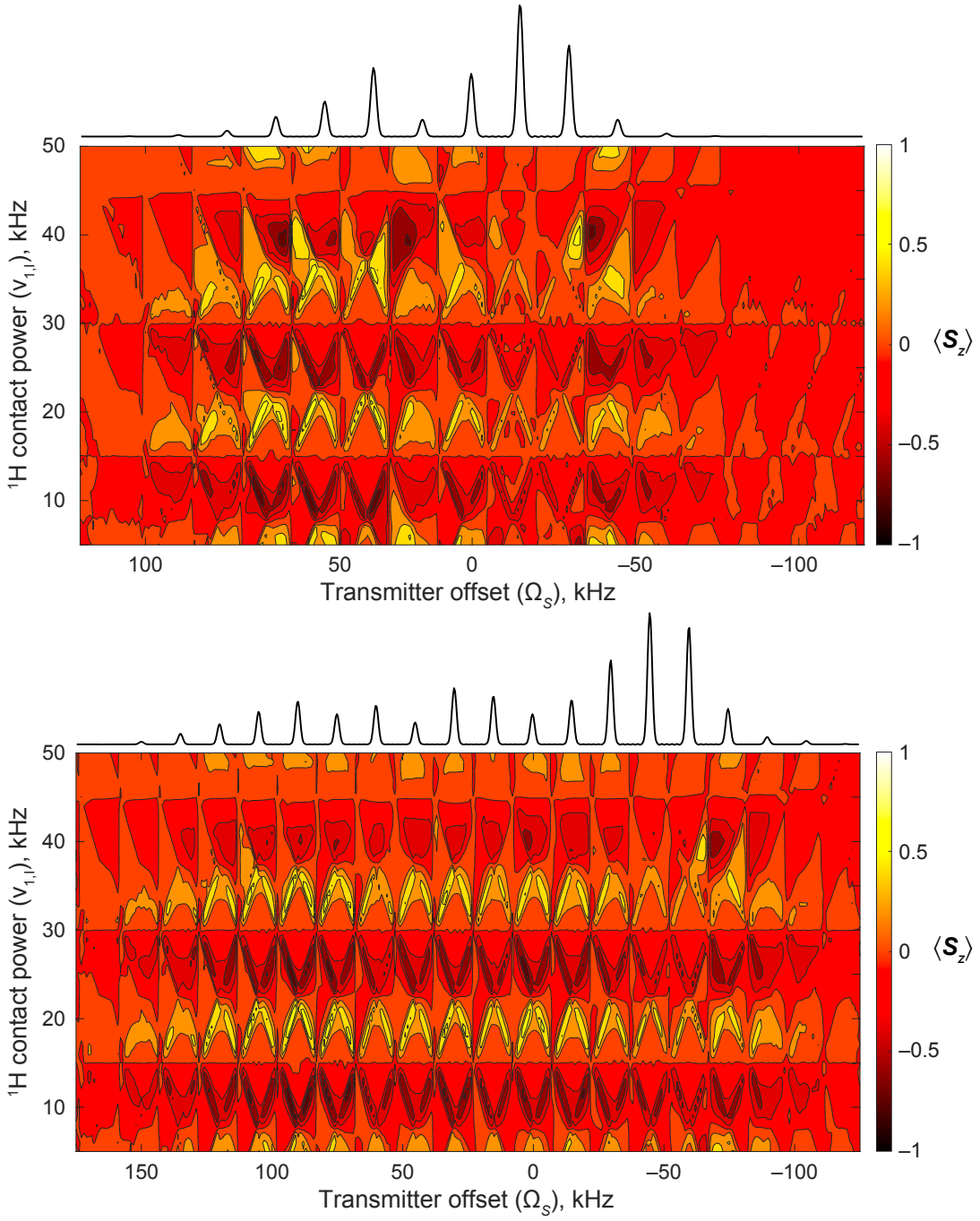

Figure S9. Numerical simulations showing the HH matching conditions for BRAIN-CP/MAS polarization transfer for a two-spin system. The ^{13}C chemical shift tensor parameters are $\delta_{iso} = 0$ ppm, $\kappa = -1$, and (a) $\Omega_{CS} = 675$ ppm and (b) $\Omega_{CS} = 1350$ ppm. The expectation value $\langle \mathbf{S}_z \rangle$ is plotted as a function of $\nu_{1,I}$ and $\Omega_S/2\pi$ and powder averaged with the REPULSION scheme. Maximum signal is indicated by dark red (positive) and blue (negative) regions. The ideal MAS SSB manifold is presented above each contour plot. In all cases, $\Delta = \nu_{1,S} = \nu_{rot} = 15$ kHz and $\tau_{CT} = 10$ ms. The heteronuclear dipolar coupling is given by $b_D^{IS}/2\pi = 4$ kHz with the dipolar vector oriented at $\theta = 45°$ relative to the rotor.

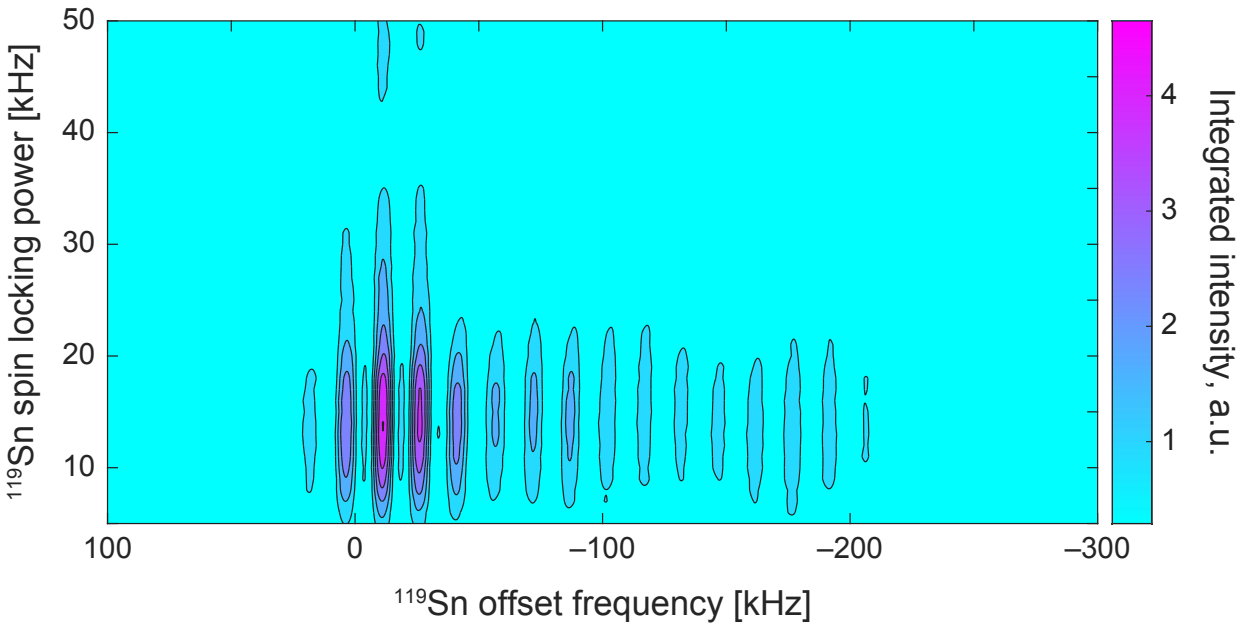

Figure S10. Contour plot showing a birds eye view of ^{1}H-^{119}Sn BRAIN-CP/WCPMG-MAS powder patterns of [Sn(HPDABA)]Cl_2 acquired at 14.1 T as a function of $\nu_{1,S}$. In all cases, ν_{rot} = Δ = 15 kHz, $\nu_{1,I}$ = 34 kHz, and τ_{CT} = 10 ms. Regions of high signal intensity are colored in pink, whereas regions of low to negligible signal intensity are light blue. Maximum signal is obtained when $\nu_{1,S} \approx \nu_{rot}$, supporting the validity of the condition expressed by **eq. 3** of the main text.

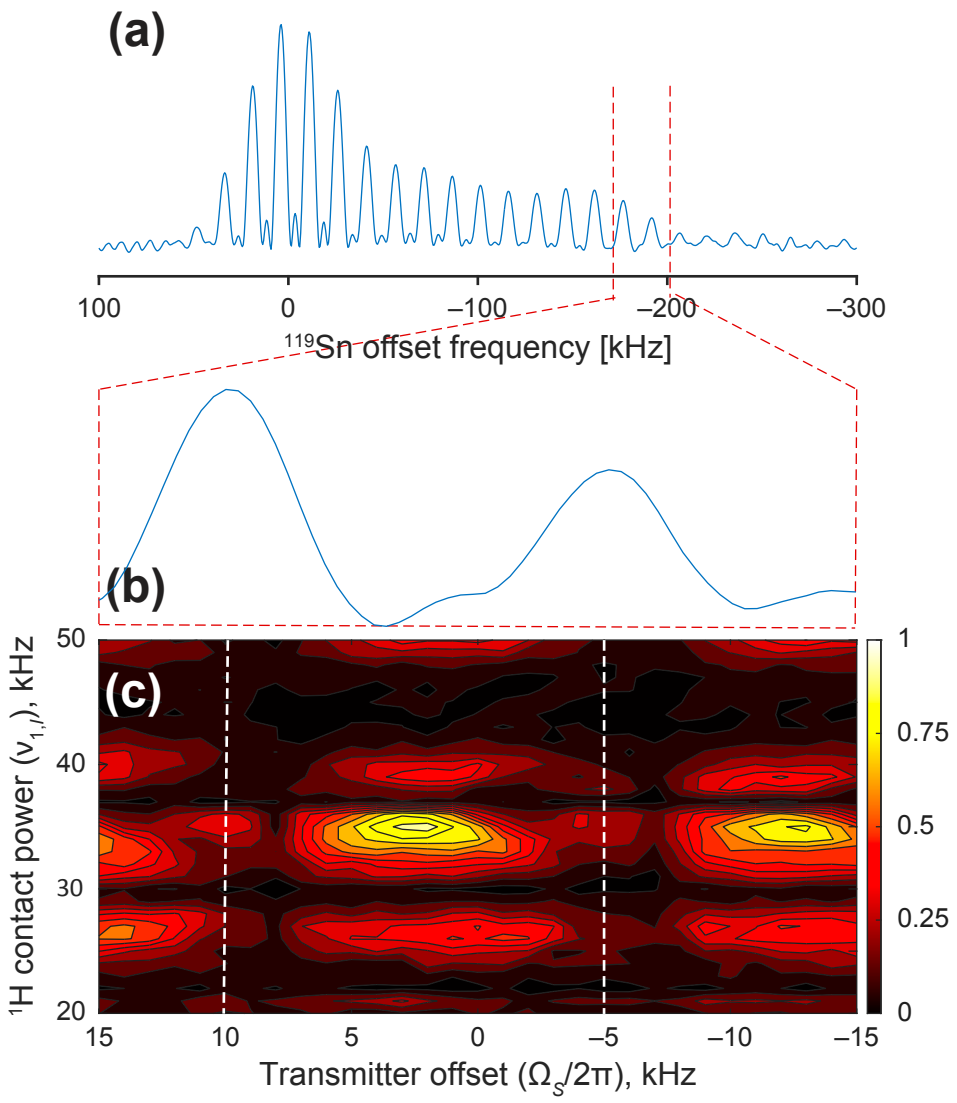

Figure S11. (a) ^{1}H-^{119}Sn BRAIN-CP/WCPMG-MAS spectrum of [Sn(HPDABA)]Cl_2 acquired with $\nu_{1,S} = \Delta = \nu_{rot} = 15$ kHz and $\nu_{1,I} = 28$ kHz. (b) Expansion of the frequency region denoted in (a) by dashed red lines. (c) Contour plot showing integrated intensities of ^{1}H-^{119}Sn BRAIN-CP/MAS spectra of [Sn(HPDABA)]Cl_2 acquired as a function of $\Omega_S/2\pi$ and $\nu_{1,I}$. The white dashed lines indicate the frequencies of the relevant SSBs.

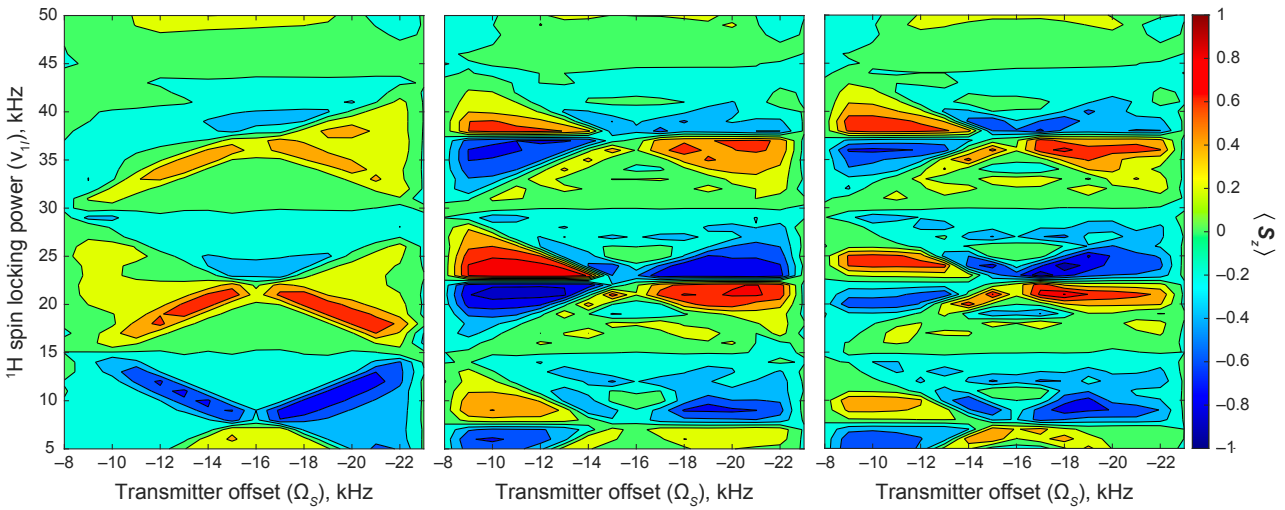

Figure S12. Numerical simulations of the HH matching conditions for BRAIN-CP/MAS polarization transfer using a (a) two-, (b) three-, and (c) four-spin system (one ^{13}C and corresponding number of ^{1}H nuclei) at ν_{rot} = 15 kHz. All parameters are identical to those of **Fig. 5** of the main text, with the addition of protons such that heteronuclear dipolar couplings as described by $b_D^{IS}/2\pi$ are set between 2 and 4 kHz and homonuclear dipolar couplings as described by $b_D^{II}/2\pi$ are set between 10 and 15 kHz.

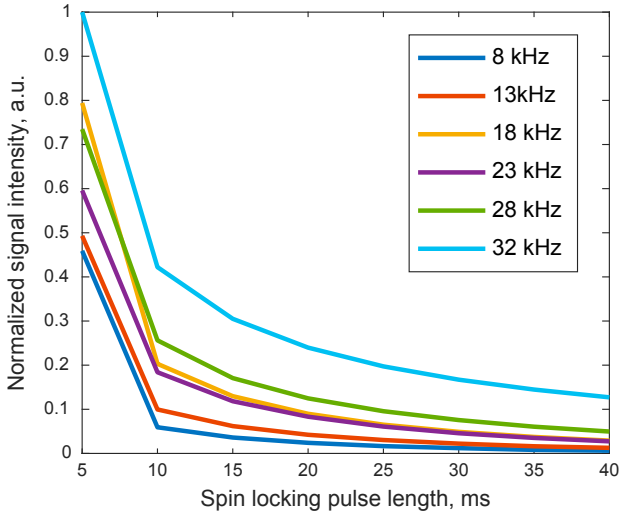

Figure S13. Integrated intensities of ^{1}H signals of [Sn(HPDABA)]Cl_2 acquired at 14.1 T at ν_{rot} = 15 kHz. Signal is acquired by a Bloch decay followed by a spin locking pulse of varying lengths and RF amplitudes, as indicated. Integrated intensities are normalized with respect to that obtained with a spin locking pulse of 5 ms and an RF amplitude of 32 kHz.

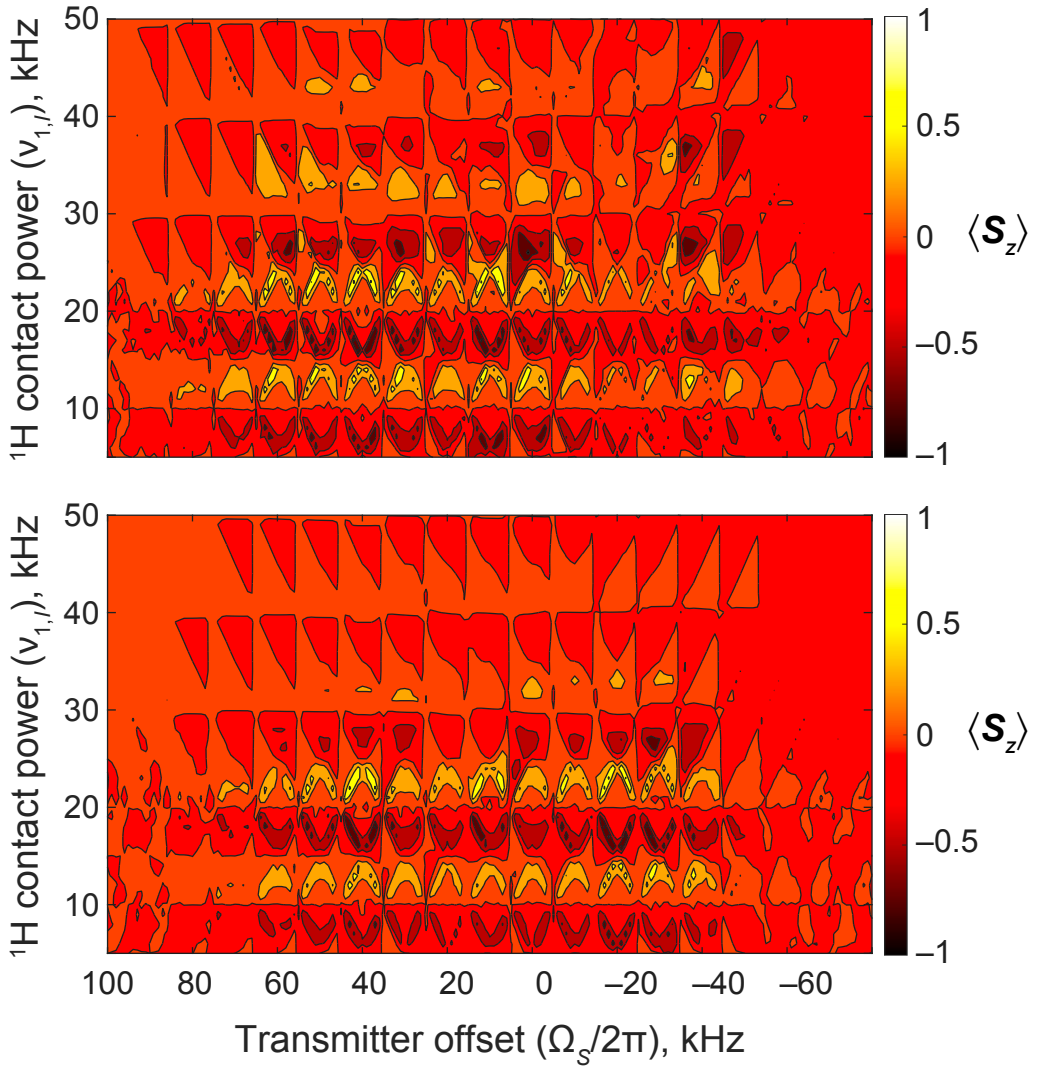

Figure S14. Numerical simulations of demonstrating the HH matching conditions for $I \rightarrow S$ BRAIN-CP/MAS transfer for a two-spin system ($I = {}^1$H, $S = {}^{13}$C) under MAS conditions of ν_{rot} = 10 kHz. The ^{13}C chemical shift tensor parameters are: δ_{iso} = 0 ppm, κ = –1, and Ω_{CS} = 675. The expectation value $\langle \mathbf{S}_z \rangle$ is plotted as a function of $\nu_{1,I}$ and $\Omega_S/2\pi$ and powder averaged with the REPULSION scheme. Maximum signal is indicated by the dark red (positive) and dark blue (negative) regions. In both panels $\Delta = \nu_{rot}$ = 10 kHz and $\nu_{1,S}$ = 10 kHz (top panel) and $\nu_{1,S}$ = 5 kHz (bottom panel). The contact time τ_{CT} is 10 ms and the heteronuclear dipolar coupling is given by $b_D^{IS}/2\pi$ = 4 kHz with the dipolar vector oriented at θ = 45° relative to the rotor.

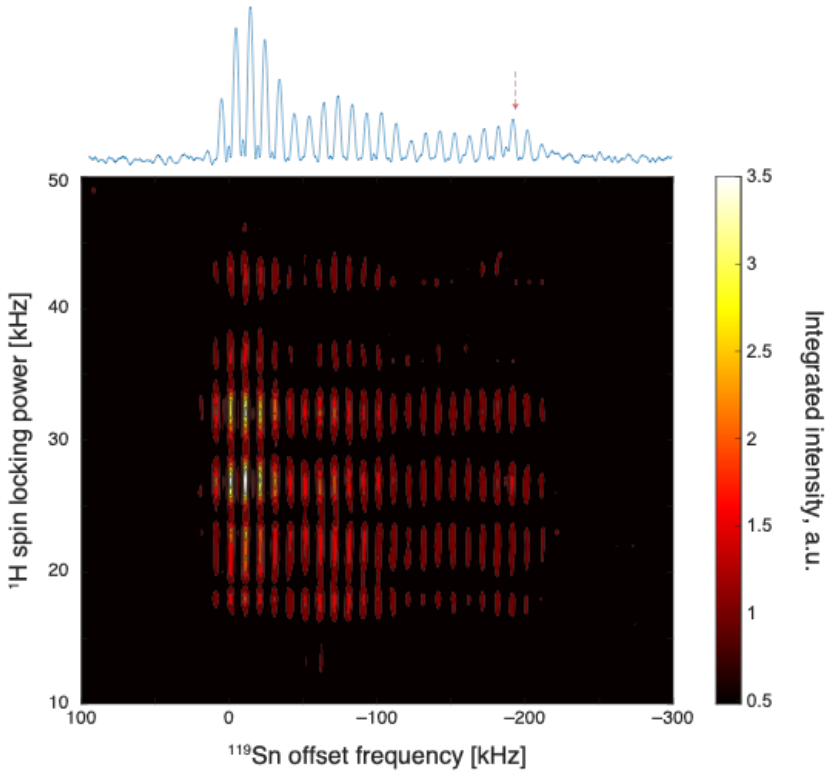

Figure S15. Contour plot showing ^{1}H-^{119}Sn BRAIN-CP/WCPMG-MAS powder patterns of [Sn(HPDABA)]Cl_2 acquired at 14.1 T as a function of $\nu_{1,I}$. The condition $\nu_{1,S} = \nu_{rot} = \Delta = 10$ kHz was in place. The spectrum shown above the contour plot was acquired with $\nu_{1,I} = 28$ kHz. The dotted red arrow indicates the value of Ω_S.

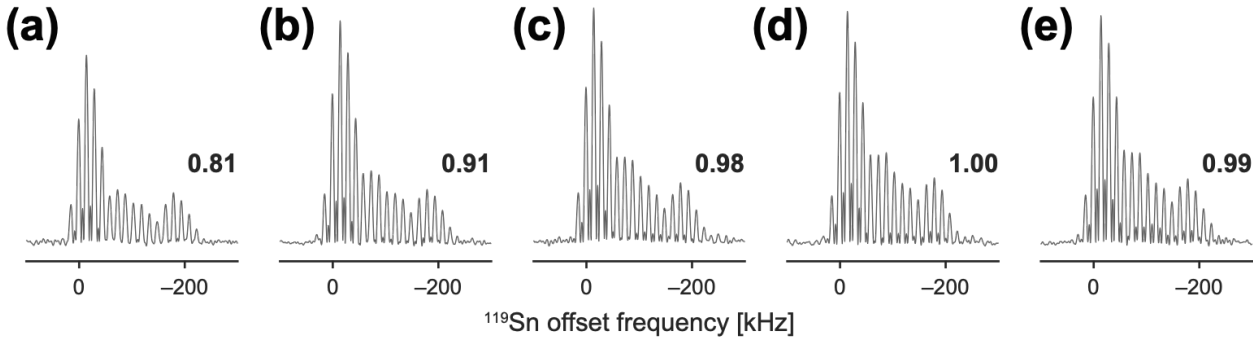

Figure S16. ^{1}H-^{119}Sn BRAIN-CP/WCPMG-MAS powder patterns of [Sn(HPDABA)]Cl_2 acquired at 14.1 T with $\nu_{1,S} = \nu_{rot} = \Delta =$ 15 kHz and τ_{CT} = (a) 5 ms, (b) 10 ms, (c) 15 ms, (d) 20 ms, and (e) 30 ms. For each experiment, the total acquisition time was held constant at 30 ms by varying the number of CPMG loops. Integrated intensities of each powder pattern are displayed in bold and normalized with respect to the pattern in (d). All patterns are plotted on the same relative intensity scale.

Pulse program for BRAIN-CP/MAS pulse sequence for Simpson simulations

```
spinsys {
  channels 13C 1H
  nuclei 13C 1H
  shift 1 0p 900p 0 0 0 0
  dipole 1 2 -4000 0 45 0
}

par {
  crystal_file     alpha0beta0
  #variable rfH     25000
  variable rfX     15e3
  #variable off     32e3
  variable ct      10000
  #variable sweep   15e3
  spin_rate        15e3
  gamma_angles     1
  variable index   1
  conjugate_fid    false

  sw               1e6
  variable tsw     1e6/sw
  np               1
  proton_frequency 600e6
  start_operator   I2x
  detect_operator  I1z
  method           direct
  verbose          1101
}

proc pulseq {} {
  global par
  offset $par(off) 0
  pulse_shaped $par(ct) $par(pulse1) $par(pulse2)
  acq
}

proc main {} {
  global par
    set start_power 5
    set end_power 50
    set start_off -20
    set end_off 20

    set shp1 [load_shape W_10ms_15kHz_20k_HtoL.txt]
```

```
   set par(pulse1) [shape_dup $shp1 0 $par(rfX)]

   for {set m $start_power} {$m <= $end_power} {incr m} {
     for {set n $start_off} {$n <= $end_off} {incr n} {
       set shp2 [load_shape square_20k.txt]
       set par(off) [expr 1e3*$n]
       set par(rfH) [expr 1e3*$m]
       set par(pulse2) [shape_dup $shp2 0 $par(rfH)]
       set f [fsimpson]
       set par(rfH_name) $m
       set par(off_name) $n
       fsave $f bcp_beta_0_H_$par(rfH_name)_$par(off_name).fid
       free_all_shapes
     }
  }
}
```

References

(1) Mehring, M. *Principles of High Resolution NMR in Solids*; Springer Berlin Heidelberg: Berlin, Heidelberg, **1983**.
(2) Mueller, L. J. *Conc. Magn. Reson. Part A Bridg. Educ. Res.* **2011**, *38 A*, 221.
(3) Edén, M. *Conc. Magn. Reson. Part A Bridg. Educ. Res.* **2003**, *17*, 117.
(4) Pell, A. J.; Kervern, G.; Emsley, L.; Deschamps, M.; Massiot, D.; Grandinetti, P. J.; Pintacuda, G. *J. Chem. Phys.* **2011**, *134*, 1.
(5) Pell, A. J.; Pintacuda, G.; Emsley, L. *J. Chem. Phys.* **2011**, *135*.
(6) Harris, K. J.; Lupulescu, A.; Lucier, B. E. G.; Frydman, L.; Schurko, R. W. *J. Magn. Reson.* **2012**, *224*, 38.
(7) Kimball, J. J.; Altenhof, A. R.; Jaroszewicz, M. J.; Schurko, R. W. *J. Phys. Chem. A* **2023**, *127*, 9621.